Geosynthetics: Leading the Way to a Resilient Planet – Biondi et al (eds)

Hyperbolic models to represent the effect of mechanical damage and abrasion on the short-term tensile response of a geocomposite

G. Lombardi & M. Pinho-Lopes
RISCO, University of Aveiro, Aveiro, Portugal

A.M. Paula
Instituto Politécnico de Bragança, Bragança, Portugal
RISCO, University of Aveiro, Aveiro, Portugal

A. Bastos
TEMA, University of Aveiro, Aveiro, Portugal
LASI, University of Minho, Guimarães, Portugal

ABSTRACT: The objective of this study was to analyse the short-term tensile response of a geocomposite (a geotextile and a geogrid overlapped) and apply hyperbolic models to describe its load-strain tensile curves. Data from specimens submitted to mechanical damage, abrasion, and mechanical damaged followed by abrasion were analysed. Reduction factors were proposed by comparing data from damaged specimens with those from undamaged specimens. The experimental results were compared with those fitted by the constitutive models to validate the model. The constitutive models demonstrated good fitting capacity. For any mechanical condition, the model parameters could be estimated by relating the experimental tensile properties of the geocomposite with adjustment coefficients, which allowed for describing the tensile load-strain curves with good accuracy. The reduction factors for the specimens subjected to mechanical damage followed by abrasion were lower than the values which would be obtained if the damages were considered individually.

1 BACKGROUND

The mechanical response of geosynthetics combines the typical behaviour of an elastic solid, viscous liquid, and plastic, and depends mostly on the temperature (McGown et al. 2004). Determining the behaviour of geosynthetics is a complex task due to several variables involve, such as environmental conditions, type of polymer, soil confinement, and level, rate and duration of loading (Greenwood et al. 2012). The performance of geosynthetics deteriorates with time due to changes in mechanical properties before, during and after installation (Shukla 2016).

Assessment of durability is based on experimental observations and tests performed to simulate damages and degradation expected during the design life of a geosynthetic. Among the durability mechanisms for soil reinforcement, tensile creep, abrasion and damage associated with installation stand out (Greenwood et al. 2012). The effects of mechanical damage on geosynthetics may be assessed by performing field tests or inducing damage in a laboratory. Mechanical damage associated with installation is relevant for all applications of geosynthetics; it has been reported by several authors, e.g Fleury et al. (2019), Domiciano et al. (2020) and Lombardi et al. (2022). Continuous dynamic loading may cause abrasion damage, as in coastal protection and road applications (Greenwood et al. 2012). The effects

DOI: 10.1201/9781003386889-287

of abrasion on the tensile response of geosynthetics were reported by different authors, e.g. Huang et al. (2007) and Pinho-Lopes & Lopes (2015).

Allen & Bathurst (1994) stated that the tensile load-strain curve of a damaged geosynthetic (Y) can be obtained using scaling factors applied to the tensile load-strain curve of the undamaged geosynthetic (X), and then drawing the remaining parts of the damaged curve parallel to the undamaged one, as illustrated in Figure 1a. In this sense, the ultimate tensile strength (T_{max}) is adjusted by R_T (Equation 1), the strain at maximum load (ε_{Tmax}) is scaled by R_ε (Equation 2), whereas the secant stiffness (J) is adjusted by R_J (Equation 3). The reduction factors RF_T, RF_ε, RF_J are defined as the inverse of R_T, R_ε and R_J respectively; RF_T is most commonly applied in the design of geosynthetics for soil reinforcement, as indicated in EN ISO 20432 (ISO 2007).

$$R_T = \frac{T_{\max}(Y)}{T_{\max}(X)} = \frac{1}{RF_T} \tag{1}$$

$$R_\varepsilon = \frac{\varepsilon_{T_{\max}}(Y)}{\varepsilon_{T_{\max}}(X)} = \frac{1}{RF_\varepsilon} \tag{2}$$

$$R_J = \frac{J_{sec}(Y)}{J_{sec}(X)} = \frac{1}{RF_J} \tag{3}$$

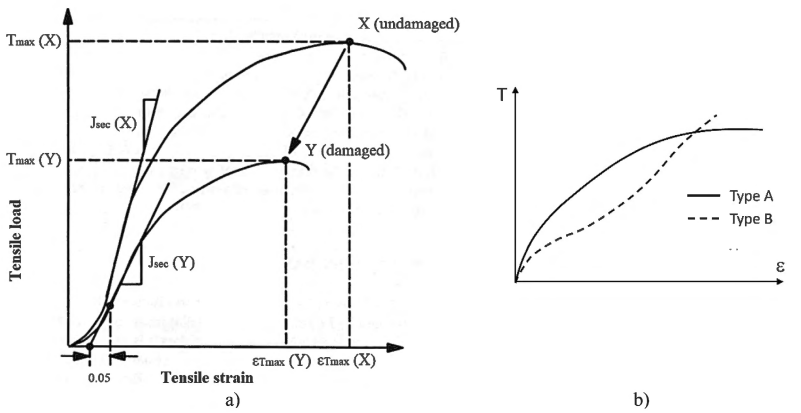

Figure 1. a) Illustration of changes in load-strain response after damage (Allen & Bathurst 1994) – adapted; b) Typical tensile load-strain curves of geosynthetics (Paula & Pinho-Lopes 2018).

According to Liu & Ling (2006), short-term load-strain curves can be fitted by hyperbolic-based models depending on the tensile response of the geosynthetic: Equation 4 for a response of type A, and Equation 5 for a response of type B, as shown in Figure 1b. For type B geosynthetics, the nonlinear function combines a hyperbola for low strains with an exponential function for high strains. The tangent stiffness J_A and J_B are given by Equations 6 and 7. T_{max} is given by Equation 8 when ε tends to ε_{Tmax}. The initial stiffness (J_i) given by Equation 9 is obtained by imposing boundary conditions on Equations 6 and 7. As reported by Lombardi et al. (2022), the adjustment coefficients C_T and C_J are included in Equations 8 and 9, respectively, in order to relate the experimental properties with the corresponding model parameters.

$$T_A = \frac{\varepsilon}{a + b \cdot \varepsilon} \tag{4}$$

$$T_B = \frac{\varepsilon}{a + 2b\varepsilon} + \frac{1}{2b} \cdot e^{-c[\varepsilon - \varepsilon_{\max}]^2} \tag{5}$$

$$J_A = \frac{dT_A}{d\varepsilon} = \frac{a}{(a + b \cdot \varepsilon)^2} \tag{6}$$

$$J_B = \frac{dT_B}{d\varepsilon} = \frac{a}{(a + 2b\varepsilon)^2} - \frac{c[\varepsilon - \varepsilon_{\max}]}{b} \cdot e^{-c[\varepsilon - \varepsilon_{\max}]^2} \tag{7}$$

$$T_{\max} = C_T \frac{1}{b} \; \varepsilon \to \varepsilon_{T_{\max}} \tag{8}$$

$$J_i = C_J \frac{1}{a} \; \varepsilon \to 0 \tag{9}$$

where a, b and c = parameters of the constitutive models.

2 MATERIALS AND METHODS

The geocomposite (GCR) studied was formed by overlapping a PET woven geogrid (GGR) on a PP nonwoven geotextile (GTX), of which the nominal properties are presented in Table 1. The test procedures adopted were the ones reported by Rosete et al. (2013). The tensile strains were measured using a video extensometer, and the full tensile load-strain curves were available. The geocomposite presented two peaks of strength, but only the first was considered.

Table 1. Nominal properties of the geosynthetics used to form the geocomposite.

Property			Geotextile (GTX)	Geogrid (GGR)
Structure			Nonwoven	Woven
Constituent polymer			PP	PET
Ultimate tensile strength[a]	T_{nom}	kN/m	55	55
Strain at maximum load[b]	ε_{nom}	%	105.0	10.5
Mass per unit area[d]	μ_{nom}	g/m^2	1000	–
Thickness[e]	t_{nom}	mm	7.2	1.7
Grid spacing	–	mm^2	–	25 x 25

[a]EN ISO 10319 [b]EN ISO 11058 [c]EN ISO 12956 [d]EN ISO 9864 [e]EN ISO 9863-1

Some specimens of the geocomposite were damaged by synthetic aggregates at 1 Hz for 200 loading cycles ranging from 5 kPa to 500 kPa (EN ISO 10722:2019). Another group of specimens was damaged by abrasion using a P100 abrasive (EN ISO 13427:1998), and another one was submitted to mechanical damage followed by abrasion. For each mechanical condition, five specimens were subjected to wide-width tensile tests (EN ISO 10319:2015), and the results were used to characterize the tensile properties of the material, namely: $J_{0.5\%}$ and $J_{2\%}$ (secant stiffness for 0.5% and 2% strain, respectively), T_{max} and ε_{Tmax}. Due to the difficulty to obtain reliable data at the beginning of the tests, herein experimental J_i was adopted as experimental $J_{0.5\%}$.

Data from damaged specimens were compared with those from undamaged specimens so that reduction factors were proposed. The reduction factor for the mechanical damage followed by abrasion was compared with those obtained by multiplying the individual reduction factors to assess the synergy between them.

Curve fittings were performed in SPSS® based on the tensile response: type A or type B; intact specimens (INT) and specimens after mechanical damage (MEC) presented a response of type B,

whereas specimens after abrasion (ABR) and mechanical damage followed by abrasion (M + A) presented a response of type A. The parameter estimates were given with 95% confidence bounds using nonlinear regressions. The adjustment coefficients were determined by linear regressions between experimental tensile properties and model parameters from curve fittings, as per Equations 8 and 9. Once C_T and C_J were determined, the model parameters were estimated by relating the experimental tensile properties and the adjustment coefficients using Equations 8 and 9.

3 RESULTS – ANALYSIS AND DISCUSSIONS

The mean experimental and fitted tensile properties are summarized in Table 2. The mean estimates of the model parameters a, b and c are given in Table 3. Table 4 gives the reduction factors (Eq. 1–3), as well as the adjustment coefficients C_T and C_J (Eq. 8 and 9). Table 3 gives the model parameters a^* and b^* estimated relating experimental J_i and C_J, and experimental T_{max} and C_T, respectively. Table 4 gives the tensile properties $T_{max}{}^{\#}$ and $J_i^{\#}$ estimated using C_T and C_J and the model parameters b and a, respectively. The experimental and fitted tensile load-strain curves are shown in Figure 2, in which the curves were plotted using the parameters a and b, and a^* and b^*.

Table 2. Mean experimental and fitted tensile properties.

	Experimental mean value								Fitted mean value				
Sample	T_{max} kN/m	CV %	ε_{Tmax} %	CV %	$J_{0.5\%}$ kN/m	CV %	$J_{2\%}$ kN/m	CV %	Fit	T_{max} kN/m	CV %	$J_{2\%}$ kN/m	CV %
INT		11	14.4	8	778.8	7	614.4	8	H_B	55.79	11	578.6	8
MEC	44.56	7	12.9	4	683.1	11	485.3	11	H_B	43.12	6	471.8	8
ABR	24.92	10	11.0	15	352.9	17	386.1	12	H_A	24.48	11	294.1	12
M + A	20.77	9	10.2	12	406.9	13	392.3	8	H_A	20.36	10	289.7	8

CV = coefficient of variation H_A = type A hyperb. model H_B = type B hyperbolic-based model

Table 3. Mean parameter estimates.

	Curve fitting								Equation 9		Equation 8	
Sample	a m/kN	CV %	b m/kN	CV %	c –	CV %	Ji kN/m	CV %	a^* m/kN	CV %	b^* m/kN	CV %
INT	0.116	7	0.016	12	0.025	42	863.38	8	0.116	7	0.016	11
MEC	0.128	13	0.021	6	0.036	10	791.84	12	0.127	11	0.020	6
ABR	0.274	21	0.016	30	–	–	377.12	20	0.271	18	0.015	11
M + A	0.220	15	0.028	18	–	–	463.44	16	0.218	12	0.027	9

$a^* = C_J / J_i$ $b^* = C_T / T_{max}$ J_i *and* T_{max} = *experimental values*

Table 4. Reduction factors, adjustment coefficients and estimated tensile properties.

	Reduction factor				Equation 8		Equation 9	
Sample	RF_T –	RF_ε –	RF_{Ji} –	$RF_{J2\%}$ –	C_T –	$T_{max}{}^{\#}$ kN/m	C_J –	$J_i^{\#}$ kN/m
INT	–	–	–	–	0.8995	55.78	0.9018	778.60
MEC	1.27	1.12	1.14	1.27	0.9051	43.13	0.8618	682.41
ABR	2.27	1.31	2.21	1.59	0.3687	23.85	0.9321	351.51
M + A	2.72	1.42	1.92	1.57	0.5467	20.12	0.8747	405.37
MxA	2.87	1.47	2.01	2.53	–	–	–	–

MxA = $RF_{(MEC)}$ x $RF_{(ABR)}$ $T_{max}{}^{\#} = C_T / b$ $J_i^{\#} = C_J / a$

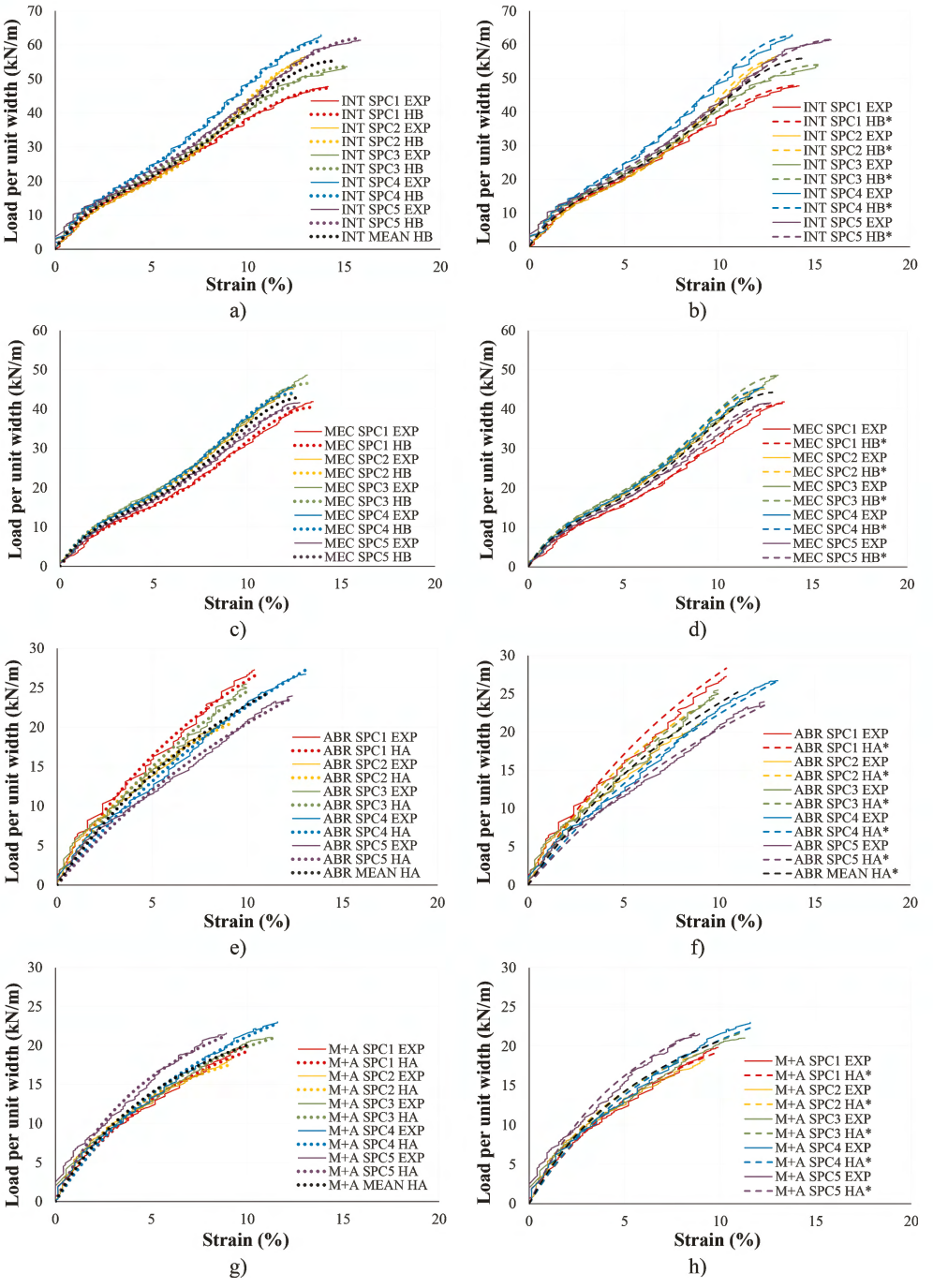

Figure 2. Experimental and fitted tensile load-strain curves of the geocomposite (GCR). a) and b): INT; c) and d): MEC; e) and f): ABR; g) and h): M + A. H_A and H_B: curves obtained using the parameters *a* and *b* from curve fitting (Table 3); HA* and HB*: curves obtained using the parameters *a** and *b**. (Table 3).

The constitutive models presented good fitting capacity, whether in terms of qualitatively describing the tensile load-strain curve or providing accurate estimates of the tensile properties. The mean curves given in Figure 2 were able to qualitatively represent the experimental curves as well as to provide accurate estimates for the tensile properties, either using mean model parameters a and b or a^* and b^*. As expected, the parameters a and b produced slightly more precise results if compared to those obtained using the parameters a^* and b^*.

Intact specimens of the geocomposite and those submitted to mechanical damage presented a type B tensile response, whereas the specimens after abrasion and mechanical damage followed by abrasion presented a type A response; thus, the effects of abrasion damage were very pronounced in the material to the extent of changing the shape of the tensile curve.

For intact and damaged specimens, the tensile properties estimated by relating the model parameters and the adjustment coefficients were notably similar to the experimental values. For any mechanical condition, the model parameters estimated by relating the experimental tensile properties of the geocomposite with the adjustment coefficients allowed for describing the tensile load-strain curves of the geocomposite with good accuracy.

The reduction factors for the specimens subjected to mechanical damage followed by abrasion were lower than those which would be obtained if the damages were considered individually, i.e. the synergy between the damage effects proved to be less harmful to the material than superimposing the effects separately, as usually done in the design of geosynthetics.

4 CONCLUSIONS

The objective of this study was to analyse the short-term tensile response of a geocomposite and apply hyperbolic models to describe load-strain tensile curves. Data from specimens submitted to mechanical damage, abrasion damage, and mechanical damage followed by abrasion were analysed. The results of the study are summarized as follows.

- The constitutive models presented good fitting capacity in terms of qualitatively describing the load-strain curve or providing accurate estimates of the tensile properties.
- Using mean model parameters to describe a representative tensile curve has shown to be effective either for the parameters a and b (curve fitting) or a^* and b^* (statistical approach).
- The tensile properties estimated by relating the model parameters and the adjustment coefficients were similar to the experimental values for intact and damaged specimens.
- The effects of abrasion damage in the geocomposite were very pronounced to the extent of changing the shape of the tensile load-strain curves.
- The reduction factors for the specimens subjected to mechanical damage followed by abrasion were lower than those which would be obtained if they were taken individually.
- The model parameters could be estimated by relating the experimental tensile properties of the geocomposite with the adjustment coefficients for intact and damaged specimens.
- Using load-strain curves after damage allows for considering realistic responses of geosynthetics in design, rather than the intact responses and reduction factors as traditionally.

ACKNOWLEDGEMENTS

This work was financially supported by: FCT (Fundação para a Ciência e a Tecnologia – Portugal) through the doctoral scholarship 2020.07874.BD (1st author) and projects UIDB/04450/2020 (RISCO), UIDB/00481/2020 and UIDP/00481/2020; PRR (Portuguese Resilience Plan through European Union – NextGenerationEU), through project TRANSFORM; Centro2020 (Centro Portugal Regional Operational Programme) through project CENTRO-01-0145-FEDER-022083.

REFERENCES

Allen, T. M., & Bathurst, R. J. (1994). Characterization of Geosynthetic Load-Strain Behavior After Installation Damage. *Geosynthetics International*, *1*(2), 181–199. https://doi.org/10.1680/gein.1.0008

Domiciano, M. L., Santos, E. C. G., & Lins da Silva, J. (2020). Geogrid Mechanical Damage Caused by Recycled Construction and Demolition Waste (RCDW): Influence of Grain Size Distribution. *Soils and Rocks*, *43*(2). https://doi.org/10.28927/SR.432231

Fleury, M. P., Santos, E. C. G., Lins Da Silva, J., & Palmeira, E. M. (2019). Geogrid Installation Damage Caused by Recycled Construction and Demolition Waste. *Geosynthetics International*, *26*(6), 641–656. https://doi.org/10.1680/jgein.19.00050

Greenwood, J. H., Schroeder, H. F., & Voskamp, W. (2012). *Durability of Geosynthetics*. CUR Building & Infrastructure.

Huang, C. C., Tzeng, Y. S., & Liao, C. J. (2007). Laboratory Tests for Simulating Abrasion Damage of a Woven Geotextile. *Geotextiles and Geomembranes*, *25*(4–5), 293–301. https://doi.org/10.1016/j.geotexmem.2007.02.008

International Organization for Standardization. (1998). EN ISO 13427:1998 – Geotextiles and Geotextile-Related Products — Abrasion Damage Simulation (sliding block test).

International Organization for Standardization. (2007). EN ISO 20432:2007 – Guidelines for the Determination of the Long-term Strength of Geosynthetics for Soil Reinforcement.

International Organization for Standardization. (2015). EN ISO 10319:2015 – Geosynthetics — Wide-Width Tensile Test.

International Organization for Standardization. (2019). EN ISO 10722:2019 – Geosynthetics — Index Test Procedure for the Evaluation of Mechanical Damage Under Repeated Loading — Damage Caused by Granular Material.

Liu, H., & Ling, H. I. (2006). Modeling Cyclic Behavior of Geosynthetics using Mathematical Functions Combined with Masing Rule and Bounding Surface Plasticity. *Geosynthetics International*, *13*(6), 234–245. https://doi.org/10.1680/gein.2006.13.6.234

Lombardi, G., Paula, A. M., & Pinho-Lopes, M. (2022). Constitutive Models and Statistical Analysis of the Short-term Tensile Response of Geosynthetics After Damage. *Construction and Building Materials*, *317*, 125972. https://doi.org/https://doi.org/10.1016/j.conbuildmat.2021.125972

McGown, A., Khan, A. J., & Kupec, J. (2004). The Isochronous Strains Energy Approach Applied to the Load-strain-time-temperature Behaviour of Geosynthetics. *Geosynthetics International*, *11*(2), 114–130. https://doi.org/10.1680/gein.2004.11.2.114

Paula, A. M., & Pinho-Lopes, M. (2018). Simple Constitutive Models to Study the Influence of Installation Damage on the Load-strain Response of Two Geogrids. *11th Internat. Conference on Geosynthetics*.

Pinho-Lopes, M., & Lopes, M. L. (2015). Synergisms between Laboratory Mechanical and Abrasion Damage on Mechanical and Hydraulic Properties of Geosynthetics. *Transportation Geotechnics*, *4*, 50–63. https://doi.org/10.1016/j.trgeo.2015.07.001

Rosete, A., Mendonça Lopes, P., Pinho-Lopes, M., & Lopes, M. L. (2013). Tensile and Hydraulic Properties of Geosynthetics after Mechanical Damage and Abrasion Laboratory Tests. *Geosynthetics International*, *20*(5), 358–374. https://doi.org/10.1680/gein.14.00015

Shukla, S. K. (2016). An Introduction to Geosynthetic Engineering. In *CRC Press.* https://doi.org/10.1201/b21582